

This article was downloaded by: [Canadian Research Knowledge Network]

On: 18 June 2011

Access details: Access Details: [subscription number 932223628]

Publisher Taylor & Francis

Informa Ltd Registered in England and Wales Registered Number: 1072954 Registered office: Mortimer House, 37-41 Mortimer Street, London W1T 3JH, UK



Journal of Earthquake Engineering

Publication details, including instructions for authors and subscription information:

<http://www.informaworld.com/smpp/title~content=t741771161>

Computational Modeling of the Seismic Performance of Beam-Column Subassemblies

G. Sagbas^a; F. J. Vecchio^b; C. Christopoulos^b

^a Halcrow Yolles, Toronto, Canada ^b Department of Civil Engineering, University of Toronto, Toronto, Canada

Online publication date: 29 April 2011

To cite this Article Sagbas, G. , Vecchio, F. J. and Christopoulos, C.(2011) 'Computational Modeling of the Seismic Performance of Beam-Column Subassemblies', Journal of Earthquake Engineering, 15: 4, 640 – 663

To link to this Article: DOI: 10.1080/13632469.2010.508963

URL: <http://dx.doi.org/10.1080/13632469.2010.508963>

PLEASE SCROLL DOWN FOR ARTICLE

Full terms and conditions of use: <http://www.informaworld.com/terms-and-conditions-of-access.pdf>

This article may be used for research, teaching and private study purposes. Any substantial or systematic reproduction, re-distribution, re-selling, loan or sub-licensing, systematic supply or distribution in any form to anyone is expressly forbidden.

The publisher does not give any warranty express or implied or make any representation that the contents will be complete or accurate or up to date. The accuracy of any instructions, formulae and drug doses should be independently verified with primary sources. The publisher shall not be liable for any loss, actions, claims, proceedings, demand or costs or damages whatsoever or howsoever caused arising directly or indirectly in connection with or arising out of the use of this material.

Computational Modeling of the Seismic Performance of Beam-Column Subassemblies

G. SAGBAS¹, F. J. VECCHIO², and C. CHRISTOPOULOS²

¹Halcrow Yolles, Toronto, Canada

²Department of Civil Engineering, University of Toronto, Toronto, Canada

Analytical studies are carried out to investigate the effectiveness of finite element modeling procedures in accurately capturing the nonlinear cyclic response of beam-column subassemblies. The analyses are performed using program Vector2, employing only default or typical material constitutive models and behavior mechanisms in order to assess analysis capabilities without the need for special modeling techniques or program modifications. The specimens considered cover a wide range of conditions, and include interior and exterior seismically and non seismically designed beam-column subassemblies. It is shown that finite element analyses can achieve good accuracy in determining the strength, deformation response, energy dissipation, and failure mode of reinforced concrete beam-column subassemblies under seismic loading conditions.

Keywords Analysis; Assessment; Beam-Column; Concrete; Finite Element; Joint; Modeling; Performance; Seismic; Retrofit

1. Introduction

Accurate performance assessment of seismically designed beam-column subassemblies has long been an important objective for researchers and designers. Experimental and analytical research on various aspects of these structural components has produced numerous design and assessment techniques, although often with little consensus. The seismic performance of non seismically designed beam-column subassemblies, commonly found in existing structures designed to obsolete codes and standards, is another challenging aspect to the problem. While research on the seismic behavior of reinforced concrete structures continues, it is nevertheless well understood that the integrity of the connection details for moment-resisting framed buildings are crucial to the survival of such structures. As observed and reported by various earthquake reconnaissance teams during site visits of seismic disaster areas, local joint failures often lead to overall structural collapse. In spite of the ductility requirements of most seismic codes, existing structures continue to fail in a brittle manner stemming from inadequate joint behavior. Insufficient reinforcement anchorage lengths, unconfined member connections, high joint shear stresses, and deficiencies in the quality of the materials are often among the main contributing factors.

In many modern design codes worldwide, seismic design provisions are increasingly requiring that designs consider the complete load-deformation response of the components rather than just designing for strength. In addition, many existing structures, including both seismically designed and non seismically designed buildings, commonly require a

Received 25 October 2009; accepted 11 July 2010.

Address correspondence to G. Sagbas, Halcrow Yolles, Toronto, Canada, M5J 1A7; E-mail: gulsah.sagbas@halcrowyolles.com

reassessment of anticipated seismic performance. Lastly, seismically deficient structures may be considered for seismic retrofitting, and alternative retrofit schemes must be investigated. In each of these three situations, the need exists for advanced analysis tools that can provide accurate assessments of the strength and performance of building components and, in particular, of seismically critical beam-column subassemblies.

2. Research Significance

In response to the need for advanced analytical tools to assist designers in undertaking comprehensive performance analyses of typical beam-column subassemblies, nonlinear finite element analysis procedures are a potentially viable option. However, such analyses can be complex, require large measures of caution and experience, and may be of questionable accuracy if not properly executed. Guidelines are required on how finite element procedures can be effectively utilized in the seismic performance analysis of beam-column subassemblies. Moreover, an objective examination of the ultimate suitability and accuracy of these methods, for such applications, is warranted. This article will attempt to fulfill these two objectives.

3. Previous Analytical Studies

Experimental and analytical research on beam-column subassemblies began in earnest in the 1970s in an effort to better understand the seismic performance of beam-column subassemblies and their contribution to the global behavior of reinforced concrete moment resisting framed buildings [e.g., Bertero and Popov, 1977; Filippou *et al.*, 1983]. Some research groups also undertook extensive research on the bond-slip behavior of deformed reinforcement in the joints, [e.g., Elieghausen *et al.*, 1983; Soroushian *et al.*, 1991], and applied these material models to the beam column models in their analytical research.

Elmorsi *et al.* [2000] proposed an inelastic plane stress element to represent the beam-column joint. This element was connected to the beams and columns with inelastic plane stress transition elements. The beams and columns were modeled with elastic beam line-elements, and inelastic truss elements. Contact elements were also used on the beam longitudinal reinforcement at the joint to represent the bond-slip effects. A smeared crack approach was used for the concrete model, and the hysteretic models were further developed to account for the shear deformations in the joint. This model successfully considered both bond-slip and shear deformation effect on beam-column subassemblies.

Limkatanyu and Spacone [2003] also studied the modeling of beam-column subassemblies. The contributions of each member to the joint were modeled separately, and members were connected with rigid links. Failure mechanisms involving shear deformations of the joint panel were neglected, and only cases with bond-slip loss within the joint were considered in this study. However, excessive shear deformations in the joint panel region were found to be critical in the seismic performance of gravity-load designed beam-column subassemblies under different frequency excitations, and it was suggested that both shear deformations and bond-slip effects should be considered, especially for medium- or low-confined joints or gravity-load designed beam-column subassemblies [fib, 2003; Dhakal *et al.*, 2005]. Celik and Ellingwood [2008] also developed a joint model based on the joint panel shear behavior for gravity-load designed RC frames, and validated their model with full-scale tests. The modeling of both joint panel shear deformations and bond-slip effects within the joints were found to be critical in the design of gravity-load designed RC frames.

Calvi *et al.* [2002] and Pampanin *et al.* [2003] suggested a section-based model that accounts for inelastic behavior mechanisms within the joints. Hysteretic response

models were refined and used for modeling a series of non seismically designed exterior beam-column subassemblies tested by Chen [2006]. Favvata *et al.* [2008] also proposed a rotational spring element to model exterior beam-column joints, and pointed to the inaccuracy of designing and modeling RC frames with the assumption of beam-column joints as rigid elements.

Lowes and Altoontash [2003] considered shear deformations and bond-slip effects within a two-dimensional beam-column joint model. Various inelastic response mechanisms such as the shear failure of the joint core, the loss of shear load transfer due to cracking at the beam-column interfaces, and the failure of the bond on the longitudinal reinforcement were also taken into account. Mitra and Lowes [2004] revised the bond-slip material and geometric behavior modeling of the previous model. Subsequent results showed that additional improvement was required with respect to bond-slip strength, particularly for the shear response of joints with low shear reinforcement ratios. Later, Mitra and Lowes [2007] improved this model to capture joint shear response, strength loss, load mechanisms, and anchorage response of interior beam-column joints. Their study also revealed the importance of bond-slip response as well as joint core response for beam-column joints.

Shiohara [2001] proposed a new model to assess the resistance mechanisms of beam-column subassemblies under seismic loading, based on a series of tests on members seismically designed according to AIJ Guidelines. This model simulated the moment effects of the beams and the columns with four triangular segments. As observed during tests, the joint shear deformations were mainly due to the diagonal cracking of the joint in the opposite directions. Two deformation modes were inherently considered: Joint Shear Mode and Beam Flexural Mode. The model was found to successfully simulate both exterior and interior seismically designed beam-column subassemblies.

Baglin and Scott [2000] and Heger *et al.* [2004] also reported successful finite element modeling of beam-column connections. These works were limited, however, to the consideration of monotonic loading conditions only. Other notable works in the field were reported by Fleury *et al.* [2000], Park [2002], Shin and LaFave [2004], and others. Most recently, MASA, a finite element code based on a micropalane material model for concrete, was used in three-dimensional modeling of non seismically designed beam-column joints [Eligehausen *et al.*, 2006, 2008]. The results of the analyses were successful in capturing the general behavior, but also indicated that significant challenges still remain with the modeling of cyclically loaded shear-critical joints.

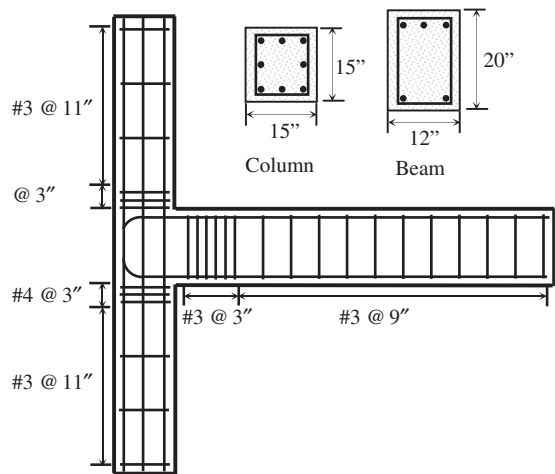
Thus, considerable progress has been made in recent years in the modeling of seismically and non seismically designed beam-column subassemblies. However, many of these studies require detailed and complex modeling processes, and are mostly applicable to specific types of beam-column joints. A need still exists for simple and generally applicable finite element procedures for the analysis of beam-column joints subjected to load reversals.

4. Guidelines for Finite Element Modeling of Beam-Column Subassemblies

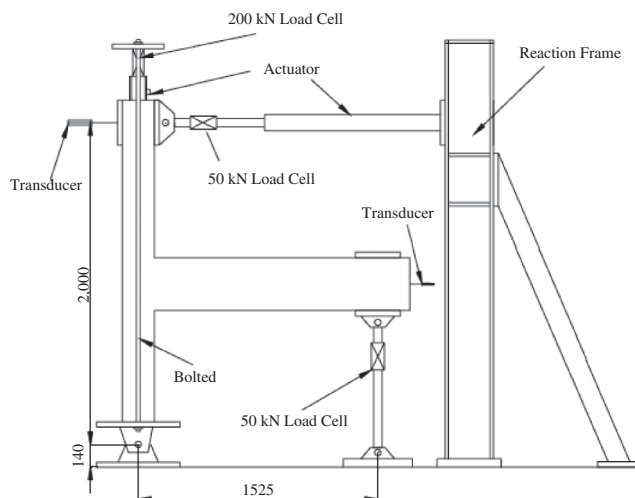
The modeling and analyses of beam-column subassemblies presented herein were carried out using the program VecTor2, a two-dimensional nonlinear finite element analysis program for reinforced concrete structures developed at the University of Toronto. An overview of the details and features of the program is provided by Wong and Vecchio [2002]. Similar advanced modeling capabilities for concrete structures are available with other specialized programs such as DIANA, Atena, COM3, FEMOOP, and MASA. (It should be noted, however, that VecTor2 is based on a smeared rotating crack model

for reinforced concrete, formulated consistent with the Disturbed Stress Field Model [Vecchio, 2000], and employs a total-load secant-stiffness algorithm. As such, it represents a substantially different procedure for finite element modeling of cyclically loaded beam-column subassemblies relative to those employed in previous studies and in the other software programs listed.) Guidelines for the general modeling of beam-column subassemblies can be distilled from the modeling techniques used in this study, discussed below.

A typical beam-column subassembly test specimen is illustrated in Fig. 1. An appropriate finite element model developed for computing the anticipated response of this specimen is shown in Fig. 2. Accurate meshing of the structure is always an important component in any finite element modeling study. It is advisable to start the modeling with a relatively

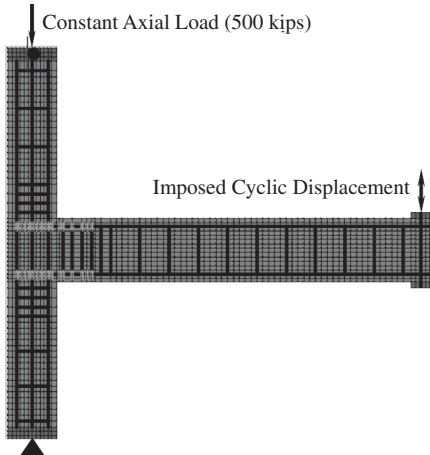


(a) Reinforcement Details

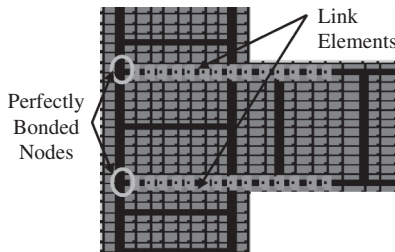


(b) Test Set-Up and Loading System [Chen, 2006].

FIGURE 1 Details of typical beam-column subassembly.



(a) Typical Meshing and Loading System of Specimen S2.



(b) Modeling of Bond-Slip Using Link Elements.

FIGURE 2 Typical finite element model of test specimen.

coarse mesh while staying true to the geometrical nuances of the structure such as rebar locations, support conditions, and loading points. This approach will lower the computation time, and will also ease the interpretation of the results. After careful examination of the results, the number of elements can be increased by using progressively finer meshes until results stabilize. Recognize that the joint panel region is where much of the governing deformation, bond-slip, yielding, and concrete damage typically occur, and it is therefore important to assign a sufficiently fine mesh to this region. In the analyses conducted in this study, where the elements used were standard plane stress rectangles (i.e., 8 dof), it was found that utilizing 12 to 15 elements through the horizontal and vertical thicknesses of the joint region provided sufficient accuracy. The concrete regions of the beam-column subassemblies were also subsequently modeled using higher-order quadrilateral elements, to allow for the consideration of nonlinear geometry effects. A comparison of the results showed no significant differences in the analysis results, and hence the simpler rectangular elements were deemed to be adequate.

Reinforcement in the specimens can be modeled using either a smeared or discrete representation. If bond-slip of the longitudinal reinforcement is to be considered, the use of discrete truss bars for the modeling of the flexural reinforcement in the beam, columns, and joint is unavoidable. If the tie reinforcement in the joint and column stubs, and the shear reinforcement in the beam, are sufficiently well distributed, then these reinforcement

components can be modeled as smeared with appropriate average reinforcement ratios defined for each particular zone of the subassembly. However, more reliable results were obtained when the transverse reinforcement, particularly in the joints, were individually represented using discrete truss bar elements. Smeared reinforcement was found to be effective in modeling out-of-plane confinement effects provided by the closed ties and stirrups, and also when modeling well-confined sections of the specimens such as where the loads or restraint conditions were introduced.

Beam-column subassemblies are subjected to severe reversed cyclic loading conditions under seismic effects. Concrete-reinforcement interactions, under these conditions, play an important role in the load transfer mechanisms that prevail. Previous research on bond-slip effects and on the seismic performance of the beam-column subassemblies have shown that “perfect bond” conditions are typically unrealistic, especially for non seismically designed structures. Therefore, an additional element at the interface between the concrete and the reinforcement elements is needed for the accurate estimation of this imperfect bonding condition. The interface element typically used is the “link” element developed by Ngo and Scordelis [1967]. Link elements are two-node non dimensional elements which consist of two orthogonal springs that connect the concrete and reinforcement elements. These two nodes can displace independently from each other, simulating the relative displacement (i.e., slip) of the reinforcement within the concrete. For example, in the typical finite element mesh shown in Fig. 2, link elements are applied to the beam longitudinal reinforcement within the column anchorage zone.

In modeling a hooked bar, a determination has to be made as to whether the hook is well anchored or not. If sufficient tie reinforcement is provided to confine the hook within the joint, then the longitudinal reinforcement can be terminated at the start of the hook and there connected with a node having “perfect bond”; i.e., the truss bar element is directly attached to the concrete at the termination point. If the hook is not well confined, as is the case in the “non seismically designed” specimens later discussed, then the imperfect bond condition modeled using link elements should be preserved at the termination point.

In all test specimens examined except Specimen S2, the seismic loading conditions were experimentally simulated using a displacement-based loading scheme with variable axial load applied to the top of the column. The restraint conditions imposed allowed the movement of the columns in the horizontal direction, but limited the vertical movement of the beams. Specimen S2 was subjected to constant axial load at the top of the column, and variable beam tip displacement. In modeling these specimens, the beam ends were restrained with pinned rollers, and steel loading plates were included on the top and bottom (see Fig. 2a). In regions where a support or load was introduced, stronger concrete was utilized to prevent any unrealistic local failure mechanisms.

5. Guidelines for Constitutive Modeling

Appropriate modeling of the constitutive response of the concrete and reinforcement, and proper consideration of important behavior mechanisms such as bond-slip and confinement, are crucial to the accurate simulation of the response of beam-column subassemblies subjected to cyclic loading. The analysis platform utilized in VecTor2 is based on a secant-stiffness total-load methodology that assumes the smeared rotating crack concept for concrete, although successful strategies can also be based on other approaches such as fixed-crack or microplane models. Here, the constitutive modeling was done according to the Disturbed Stress Field Model (DSFM) [Vecchio, 2000], which is an extension of the Modified Compression Field Theory (MCFT) [Vecchio and Collins, 1986]. Aspects of the

material modeling that were significant to the computed responses of the subassemblies examined will be briefly identified.

In elements where insufficient transverse reinforcement exists or where concrete strut action is vulnerable due to high stresses or damage, as may be the case in the joint regions of beam-column subassemblies, compression softening effects due to transverse cracking may play a significant role in limiting the strength and ductility. In addition, when attempting to accurately capture the deformation response and energy-dissipating characteristics of the overall subassembly, tension stiffening effects will play a key role. Both the compression softening effects and tension stiffening effects were modeled as presented in the DSFM.

In zones where the concrete is subjected to bi-axial or tri-axial compressive stresses, either due to the reinforcement provided or as a consequence of the loading and internal stress conditions, confinement effects will have a significant influence on the strength, ductility, failure mode, and energy-dissipation characteristics of the component. Such influences are particularly important when modeling well-confined joints. In the analyses undertaken, strength enhancement due to confinement was modeled according to the Kupfer-Richart criteria, which is a combination of a biaxial compression model by Kupfer *et al.* [1969] and a model that considers the effect of spiral reinforcement in columns by Richard *et al.* [1928]. The post-peak response was modeled according to the "modified Park-Kent model" which is the modified version of the Kent and Park [1971] stress-strain curve by Park *et al.* [1982].

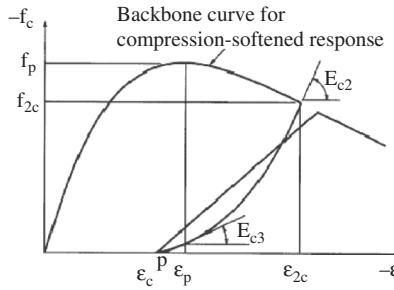
Under seismic loading conditions, a proper representation of the loading/unloading behavior and the cyclic-load induced damage sustained by the concrete is critical in determining the strength and energy-dissipation capacity of the subassembly. The hysteretic model for the concrete employed here was that proposed by Palermo and Vecchio [2003] (see Fig. 3a).

Concrete cracking was evaluated according to the Mohr-Coulomb criterion with tension cut-off. Pre-peak compression response was represented using the simple Hognestad parabola, and concrete tension softening effects were modeled using a linear decay based on a fixed fracture energy of 75 N/m. Shear slip on crack surfaces were modeled according to the Walraven [1981] formulation. Tensile cracking, tension softening, crack shear slip, and pre-peak compression response of the concrete were not significantly influencing factors.

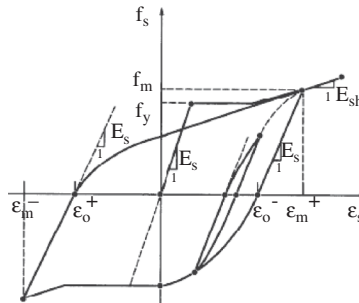
The reinforcement response was modeled using an elastic-plastic function with strain hardening. Bauschinger effects, critical in the proper evaluation of energy dissipation in subassemblies experiencing extensive yielding of the flexural reinforcement, were modeled according to the Seckin [1981] formulation (see Fig. 3b). Dowel action of the reinforcement is important in the determination of the shear strength and post-peak ductility of reinforced concrete elements containing low amounts of shear reinforcement; here, the Tassios model [1987] was used. Reinforcement compression buckling was modeled according to the Asatzu [Asatzu *et al.*, 2001] formulation.

The performance of the beam-column subassemblies are highly influenced by the bond-slip behavior of the beam longitudinal reinforcement. Modeling of the bond behavior between the concrete and the reinforcement is one of the most critical elements in a successful finite element simulation of seismic behavior. For deformed reinforcing bars, the reversed cyclic curve proposed by Eligehausen *et al.* [1983] was used (see Fig. 3c). In this model, the effects of confinement (through the use of a confinement index β calculated and input by the user), and strength damage due to cycling (through a damage index continually calculated and updated in the model) are taken into account.

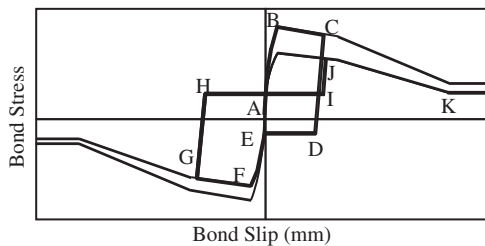
The non seismically designed subassemblies modeled in some cases consisted of smooth bars as beam longitudinal reinforcement. A provisional monotonic bond stress-slip



(a) Hysteretic Response of Concrete Based on Palermo Model [2002].



(b) Hysteretic Response of Reinforcement Based on Seckin Model [1981].



(c) Cyclic Bond Stress-Slip Model for Deformed Rebar by Eligehausen et al [1983].

FIGURE 3 Constitutive models.

formulation was derived from the work of Fabbrocino *et al.* [2004] and adapted to the cyclic loading/unloading model of Eligehausen.

All of the material models identified above and used for the analyses to follow, except for the Palermo concrete hysteretic model and the Fabbrocino bond-slip model (for smooth reinforcement), are the default options in VecTor2 (see Table 1). (The analysis results of load-deformation behavior with the default option for the concrete hysteretic model resulted in higher stiffness values compared to the experimental results. The effects of previous loading conditions, which typically result in significant plastic deformation and strength decay, were more successfully captured with the ‘Palermo (w/Decay)’ option.) Otherwise, the default models are recommended as basic constitutive models appropriate for modeling beam-column subassemblies. No attempt was made to “fine-tune” or “optimize” the analyses by selecting or implementing alternative models. Full details of all behavior models cited are provided by Wong and Vecchio [2002].

TABLE 1 Material behavior models used in modeling with VecTor2

Material Property	Model
Concrete Compression Pre-Peak Response	Hognestad Parabola
Concrete Compression Post-Peak Response	Modified Park-Kent
Concrete Compression Softening	Vecchio 1992-A (e1/e2-Form)
Concrete Tension Stiffening	Modified Bentz 2003
Concrete Tension Softening	Linear
Concrete Tension Splitting	Not Considered
Concrete Confined Strength	Kupfer/Richard Model
Concrete Dilation	Variable Kupfer
Concrete Cracking Criterion	Mohr-Coulomb (Stress)
Concrete Crack Slip Check	Vecchio-Collins 1986
Concrete Crack Width Check	Agg/5 Max Crack Width
Concrete Hysteretic Response	Palermo 2002 (w/Decay)*
Reinforcement Hysteretic Response	Seckin Model (Bauschinger)
Reinforcement Dowel Action	Tassios Model (Crack Slip)
Reinforcement Buckling	Asatzu Model
Bond Model	Eligehausen Model

*non-default model.

6. Exterior Beam-Column Subassemblies with Deformed Reinforcement

Four exterior beam-column test specimens, constructed using deformed longitudinal reinforcement, were considered. These included: S2 tested by Bond [1969] and Goyal [1969], B2 [Shiohara and Kusuvara, 2006], TDD1 and TDD2 [Chen, 2006].

Specimen S2, a full-scale model from a multi-story moment resisting frame, was designed according to the seismic requirements of ACI 318-77. (For this specimen, the loading and restraint conditions were slightly different from typical; the subassembly was subjected to constant axial load at the top of the column, and varying beam tip displacement.) The second specimen, B2, was taken from a Benchmark Study conducted by Shiohara and Kusuvara [2006]. This specimen was seismically designed according to the AIJ 1999 code specifications, and represented a $\frac{1}{2}$ -scale exterior beam-column subassembly of a typical moment resisting reinforced concrete framed building. Specimens TDD1 and TDD2 were tested by Chen [2006] at the University of Canterbury, New Zealand. These two specimens were $\frac{2}{3}$ -scale exterior beam-column subassemblies designed with structural deficiencies such as unconfined beam-column joints and low-quality concrete. Also, they did not adhere to the weak beam-strong column design philosophy for ductile failure mechanism, reflecting typical pre-1970s non seismically designed structural members. All specimens were subjected to complex loading protocols that involved variable axial loads in the columns and cyclic column tip displacements of progressively increasing amplitudes [Pampanin *et al.*, 2002]. Complete specimen details and loading conditions can be found in Sagbas [2007].

The experimentally observed failure of Specimen S2 involved extensive shear cracking at the beam-column joint. The first shear cracking was reported to have occurred during the 2nd cycle in the positive loading direction. These cracks gradually propagated through the upper and lower column, and the specimen failed with extensive cracking and concrete cover spalling in the joint [Bond, 1969; Goyal, 1969].

Specimen B2 experienced flexural cracking at the beam-column interface, and shear cracking in the joint. The first flexural and shear cracking was reported at the end of the 1.0% drift ratio cycle. The yielding of beam longitudinal reinforcement occurred between 1.0% and 2.0% drift ratios. At the 2.0% drift cycle, flexural cracks were observed at the upper and lower column ends. Horizontal cracks were reported between the two steel anchorage plates at the end of the 3.0% drift ratio cycle. Later, these cracks propagated and joined the shear cracks at the center of the joint, accompanied by the concrete cover spalling and the anchorage plate pushing off the concrete [Shiohara and Kusuvara, 2006].

Specimen TDD1 experienced large flexural cracking at the beam-column interface and concrete spalling from the back of the column at the joint. The hooked longitudinal bars lost all anchorage capacity at this point. In Specimen TDD2, a brittle joint failure mechanism was observed at the end of the testing. According to the experimental results, the first shear crack within the joint was observed at 0.65% drift in both loading directions. Later, a concrete wedge mechanism formed with the propagation of individual shear cracks at 3.0% drift [Chen, 2006].

The test specimens were modeled according to the meshing guidelines and material models discussed previously. Typical specimen details and finite element meshing are illustrated in Fig. 4. All material properties, reinforcement details, loading conditions, and support conditions were modeled consistent with the test specimen details.

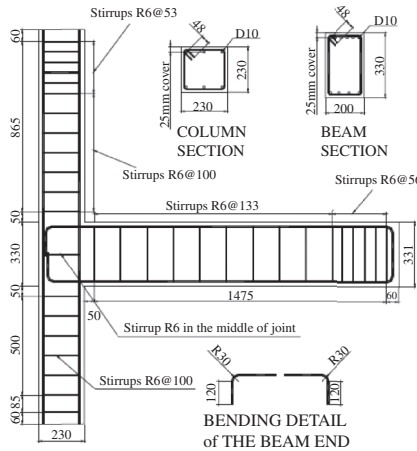
The finite element analyses were able to provide accurate simulations of the behavior and sequence of damage for all four test specimens. Comparisons of the observed and calculated load-displacement responses are given in Fig. 5; in general, good correlations were obtained although the accuracy was better with the two seismically designed specimens (i.e., S2 and B2). The sequences of cracking, yielding, spalling, and bond-slip, and the final failure modes, were typically predicted with a high degree of accuracy (e.g., see Fig. 6).

Further comparisons of calculated to observed responses are given in Table 2. With respect to strength capacity (V_{max}), the ratio of the calculated to measured peak shear force in the positive loading direction had a mean of 1.04 and a coefficient of variation of 2.3%; in the negative direction, it was 1.02 and 4.3%, respectively. Ultimate displacement ductility ratios (μ), based on the relative column tip deflections at the time of first flexural yielding, were equally well estimated. The ratio of calculated to measured total energy dissipation (ΣE), based on the total areas contained in the force-displacement hysteresis up to termination of testing, showed somewhat more scatter. But, given that an accurate estimate of total energy dissipation in elements taken to advanced stages of post-peak behavior is exceedingly difficult to achieve, particularly when two of the specimens were inadequately designed, the mean ratio of 0.98 must be considered highly satisfactory.

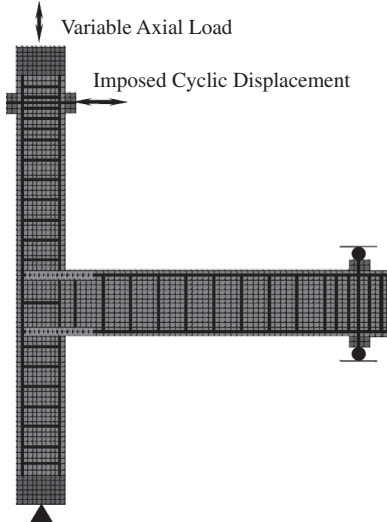
7. Interior Beam-Column Subassemblies with Deformed Reinforcement

The four $\frac{1}{2}$ -scale interior beam-column subassemblies tested by Shiohara and Kusuvara [2006] were selected for analysis; namely, Specimens A1, A2, A3, and B1. These subassemblies were seismically designed according to the AIJ 1999 code revisions, and tested under displacement-controlled reversed cyclic loading conditions. Longitudinal reinforcement and loading protocols were the primary test variables. The finite element meshes employed in modeling these specimens were of the configuration shown in Fig. 7. Note that although the beam longitudinal reinforcement was continuous through the joint regions, the possibility of bond-slip was retained in the modeling through the use of bond-link elements.

Specimen A1 experienced large shear deformations and a highly pinched hysteretic response indicative of a shear failure. Bulging of the concrete cover and crushing at the



(a) Details of Specimen TDDI Tested by Chen [2006]



(b) Finite Element Model of Specimen TDDI

FIGURE 4 Typical model of exterior beam-column subassembly.

beam end, near the joint, became apparent at 2.0% column drift. Concrete cover spalling occurred at 3.0% column drift, and severe joint deformation was visible during the last cycle at the 4.0% column drift. Extensive shear deformations were observed in the joint region, but no plastic hinging of the beams was noted [Shiohara and Kusuhara, 2006].

With Specimen A2, the main crack formation consisted of flexural cracking at the beam column interface. Flexural cracks were first seen at the beam-column interface, later followed by diagonal shear cracks in the joint region. In the latter stages of loading, the widths of the flexural cracks increased rapidly compared to those of the shear cracks at the joint. The hysteretic response of this specimen showed a symmetric and stable behavior, indicative of a flexural hinging failure [Shiohara and Kusuhara, 2006].

Specimen A3 also exhibited a stable hysteretic response indicative of a flexure-dominated failure mechanism. Both flexural and shear cracking was observed, and these

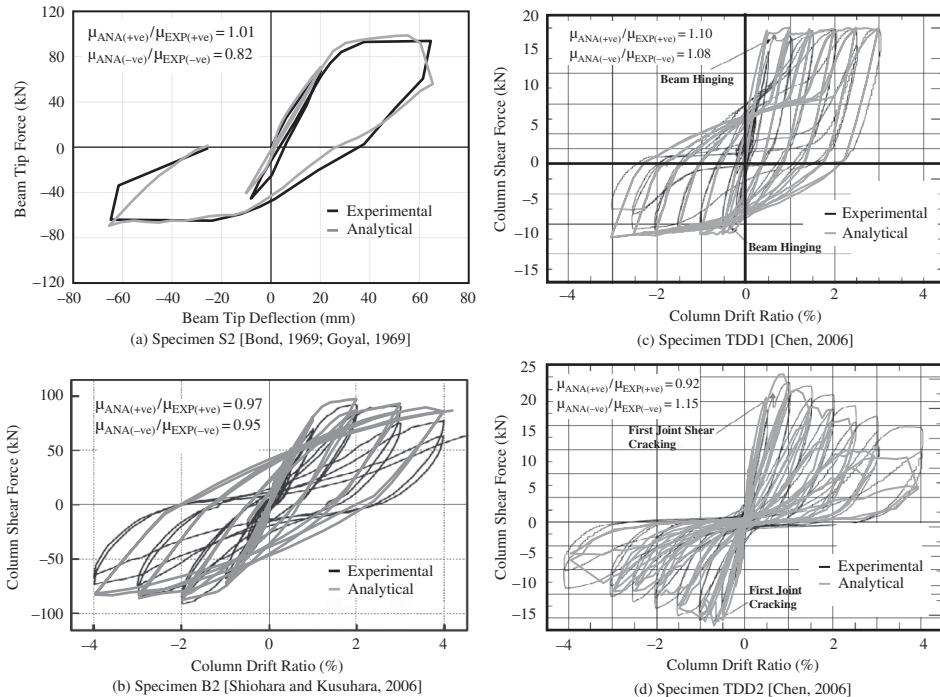


FIGURE 5 Column shear-drift response for exterior beam-column subassemblies.

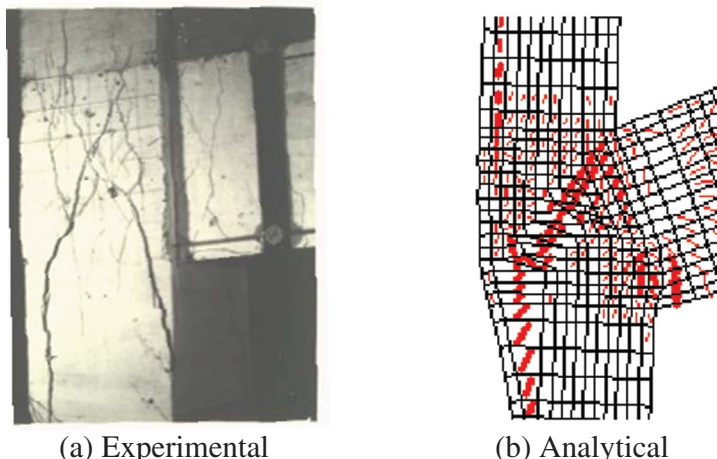


FIGURE 6 Comparison of final failure mode of Specimen S2 [Bond, 1969; Goyal, 1969] (color figure available online).

cracks gradually increased during testing. As a result of this flexural cracking, concrete spalling at the corner of the specimen was observed [Shiohara and Kusuhara, 2006].

The column shear force versus column drift response of Specimen B1 showed a moderately pinched hysteretic behavior as the specimen sustained heavy damage in the joint region. The first diagonal shear cracks were observed during the first 0.5% drift loading cycle; these cracks opened significantly during the 1.0% drift cycle. The first flexural cracks

TABLE 2 Comparison of calculated and measured responses

Specimen	Type of Joint Reinforcement	Type of Reinforcement	Failure Mechanism	Positive Loading Direction				Negative Loading Direction				
				$V_{max}^{(EXP)}$ (kN)	$V_{max}^{(VT2)}$ (kN)	$V_{max}^{(VT2)}/V_{max}^{(EXP)}$	$\mu^{(VT2)}/\mu^{(EXP)}$	$V_{max}^{(EXP)}$ (kN)	$V_{max}^{(VT2)}$ (kN)	$V_{max}^{(VT2)}/V_{max}^{(EXP)}$	$\mu^{(VT2)}/\mu^{(EXP)}$	
S2 ¹	EXT	Smooth	Joint Shear	94.0	98.0	1.04	1.01	64.9	69.3	1.07	0.82	0.98
B2 ²	EXT	Deformed	Flexural/J.Shear	92.2	95.6	1.04	0.97	91.1	88.9	0.98	0.95	0.97
TDD1 ³	EXT	Deformed	Flexural	18.0	18.0	1.00	1.10	10.0	9.8	0.98	1.08	1.27
TDD2 ³	EXT	Deformed	Joint Shear	23.0	24.5	1.07	0.92	16.0	17.0	1.06	1.15	0.70
A1 ²	INT	Deformed	Joint Shear	126.6	128.3	1.01	0.91	122.8	130.0	1.06	1.03	0.83
A2 ²	INT	Deformed	Flexural/J.Shear	77.9	79.6	1.02	1.08	77.1	70.6	0.92	1.28	1.06
A3 ²	INT	Deformed	Flexural/J.Shear	176.4	176.1	1.00	0.82	124.5	113.1	0.91	0.89	0.93
B1 ²	INT	Deformed	Flexural/J.Shear	98.1	94.9	0.97	0.85	92.6	91.0	0.98	0.85	0.98
TDP1 ³	EXT	Smooth	J.Shear/Flexural	16.3	18.4	1.13	1.26	8.9	9.4	1.06	1.15	0.60
TDP2 ³	EXT	Smooth	Joint Shear	16.2	18.6	1.15	1.09	14.0	18.8	1.34	0.93	0.60
C ⁴	INT	Smooth	Joint Shear	16.0	16.0	1.00	1.26	17.0	15.0	0.88	1.15	0.70
THR ³	EXT	Smooth	Flexural	25.5	28.6	1.12	1.09	26.2	28.7	1.10	0.93	1.42
			Mean		1.05	1.03			Mean	1.03	1.02	0.92
			St. Dev		0.06	0.14			St. Dev	0.12	0.14	0.24
			COV (%)		5.37	13.36			COV (%)	11.36	13.57	26.47

¹Bond [1969] and Goyal [1969]; ²Shiohara and Kusuhsara [2006]; ³Chen [2006]; ⁴Pamparin [2002].

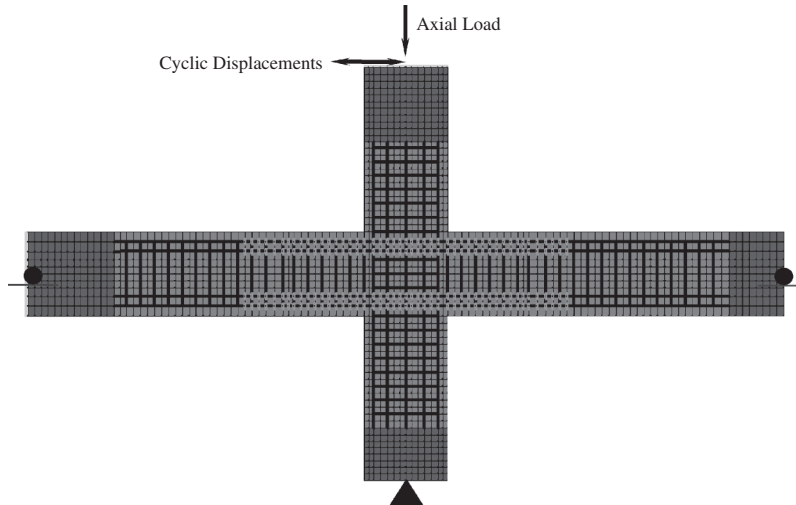


FIGURE 7 Typical finite element mesh for interior beam-column subassembly.

were seen at the end of the 1.0% drift cycle. Crushing of the concrete was severe at the beam-column joint and at the inner corners of the beam-column connection. Deformations and residual deflections increased significantly after yielding of the beam longitudinal reinforcement [Shiohara and Kusuhara, 2006].

The observed column shear vs. column drift responses for the four specimens are reproduced in Fig. 8. Also shown are the corresponding calculated responses obtained from the finite element analyses; highly accurate correlations to the experimental results

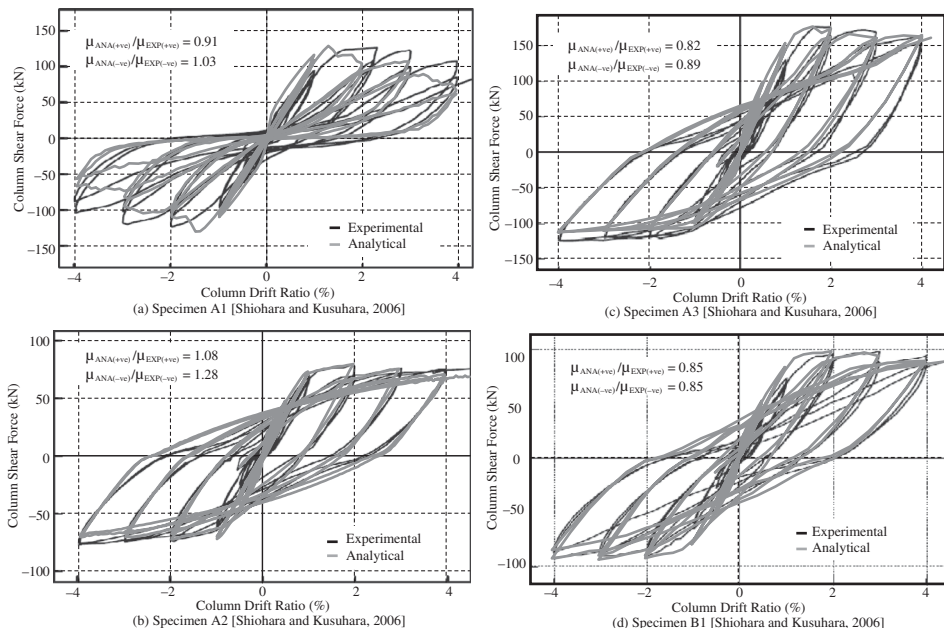


FIGURE 8 Column shear-drift response for interior beam-column subassemblies.

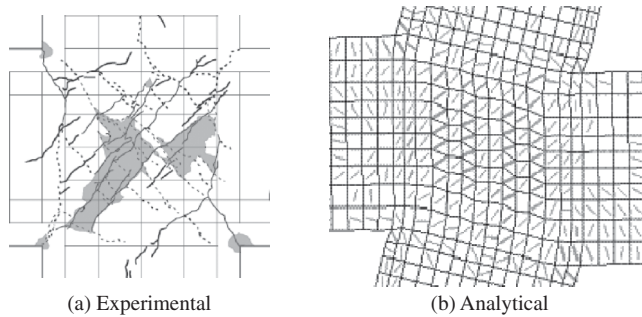


FIGURE 9 Comparison of failure mechanism for Specimen A1 at 3% drift.

are seen. The ratio of the predicted to the observed peak shear force results had a mean and coefficient of variation of 1.00 and 2.1% in the positive loading direction, 0.97 and 6.3%, in the negative loading direction (see Table 2). The displacement ductility ratios and the total energy dissipations were also well simulated (see Table 2), as were the sequences of damage and final failure mechanisms (e.g., see Fig. 9).

8. Beam-Column Subassemblies with Smooth Reinforcement

Three beam-column subassemblies constructed using non deformed (smooth) reinforcing bars for the main reinforcement were also examined: two exterior joint subassemblies (Specimens TDP1 and TDP2) tested by Chen [2006], and one interior joint subassembly (Specimen C2) tested by Pampanin *et al.* [2002]. These specimens are representative of some buildings currently in use in various seismic regions (Figs. 10, 11). They were non seismically designed; in addition to the use of smooth bars, problems existed with the reinforcement detailing such as inadequate anchorage lengths and poor confinement in the joints. For the two exterior subassemblies, the beam longitudinal bars were anchored into the joint with hooked ends but an inadequate amount of shear reinforcement was included in the joint.

In the testing of Specimen TDP1, a joint shear failure was observed in the positive loading direction, while a flexural failure at the beam-column interface was observed in the negative loading direction. In the positive loading direction, the first joint shear cracking was observed at 1.33% column drift, and the shear resistance of the member decreased after this cracking occurred. Later, the shear strength of the specimen recovered to its previous values, but then started decreasing gradually with the opening of the diagonal cracks in the joint. Beam hinging was observed only in the negative loading direction. The hysteretic response showed a pinched behavior which indicated slippage of the reinforcement [Chen, 2006].

With Specimen TDP2, a brittle joint shear failure was observed by Chen [2006]. The first joint shear cracks occurred during the 1.0% drift cycles, and gradually increased in the positive and the negative loading directions. Similar to Specimen TDP1, the hysteretic response showed a pinched behavior indicating shear-dominated behavior and likely slippage of the reinforcement. A concrete wedge failure mechanism was observed in this specimen [Chen, 2006].

The interior beam-column subassembly, Specimen C2, showed a pinched hysteretic response and failed with shear cracking at the joint. Shear cracking was first observed in the joint, followed by a drop in stiffness, at the 0.8% drift ratio. After reaching the

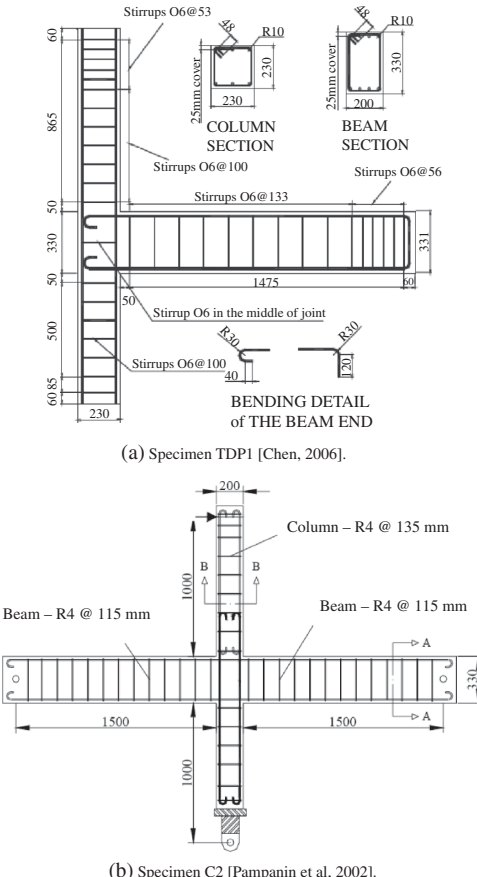
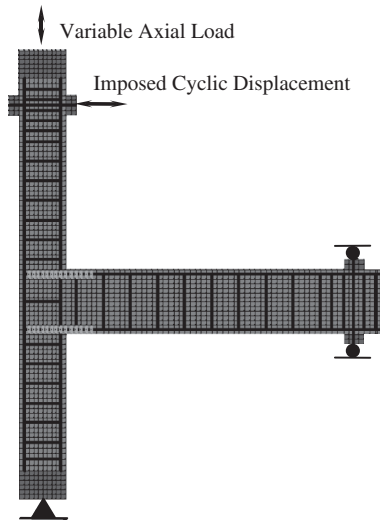


FIGURE 10 Non seismically designed subassemblies with smooth reinforcement.

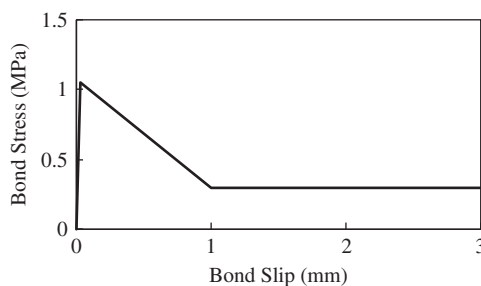
ultimate shear force value at 3.5% drift, a softening in the hysteretic response was observed. However, the specimen continued to carry a significant portion of the peak load up to the end of the experiment [Pampanin *et al.*, 2002].

These specimens were modeled in the same manner as the seismically designed specimens previously considered (see Fig. 11a), using the same material models and mesh characteristics, with one major exception. A monotonic bond stress-slip model was inferred from the work of Fabbrocino *et al.* [2004], as shown in Fig. 11b, and this model was adapted to the loading/unloading rules and damage index defined within the Eligehausen model. No cyclic bond stress-slip model for smooth bars currently exists in the literature, and the model implemented here can only be considered as cursory at best given the scarce data and tenuous assumptions on which it is based.

Generally, the analysis results provided a reasonably accurate simulation of the observed behaviors, albeit with somewhat more scatter than previously observed. The highly pinched hysteretic responses obtained, heavily influenced by shear deformation and damage in the joints and slip of the beam longitudinal reinforcement, correlate sufficiently well with the experimental responses shown in Fig. 12. The strength decay at later stages of loading was underestimated for the exterior joints and overestimated for the interior joint. In all cases, the displacement ductility was marginally overestimated,



(a) Bond-Slip Elements Used in Modeling Specimen TDP1 S



(b) Monotonic Bond Stress-Slip Response for Smooth Bars.

FIGURE 11 Bond-slip modeling of smooth bar reinforcement.

and the total energy dissipation underestimated. These deficiencies were likely the result of the bond-slip response of the smooth bars under cyclic loading not being well captured by the Eligehausen model which was developed for deformed rebars. Nevertheless, the correct cracking patterns and modes of failure were obtained from the analyses; for example, as seen in Fig. 13, a concrete wedge failure mechanism with punching out of the beam top reinforcing bars was correctly determined for Specimen TDP2. Comparisons of the predicted-to-observed shear capacities, ductility ratios, and total energy dissipation are given in Table 2.

9. Retrofitted Exterior Beam-Column Subassembly

The final specimen examined, Specimen THR, was an exterior beam-column subassembly retrofitted in accordance with a new technique developed by Pampanin *et al.* [2006]. The retrofit technique was developed with the aim of transforming the unwanted brittle failure mechanism common in non seismically designed beam-column subassemblies to a more

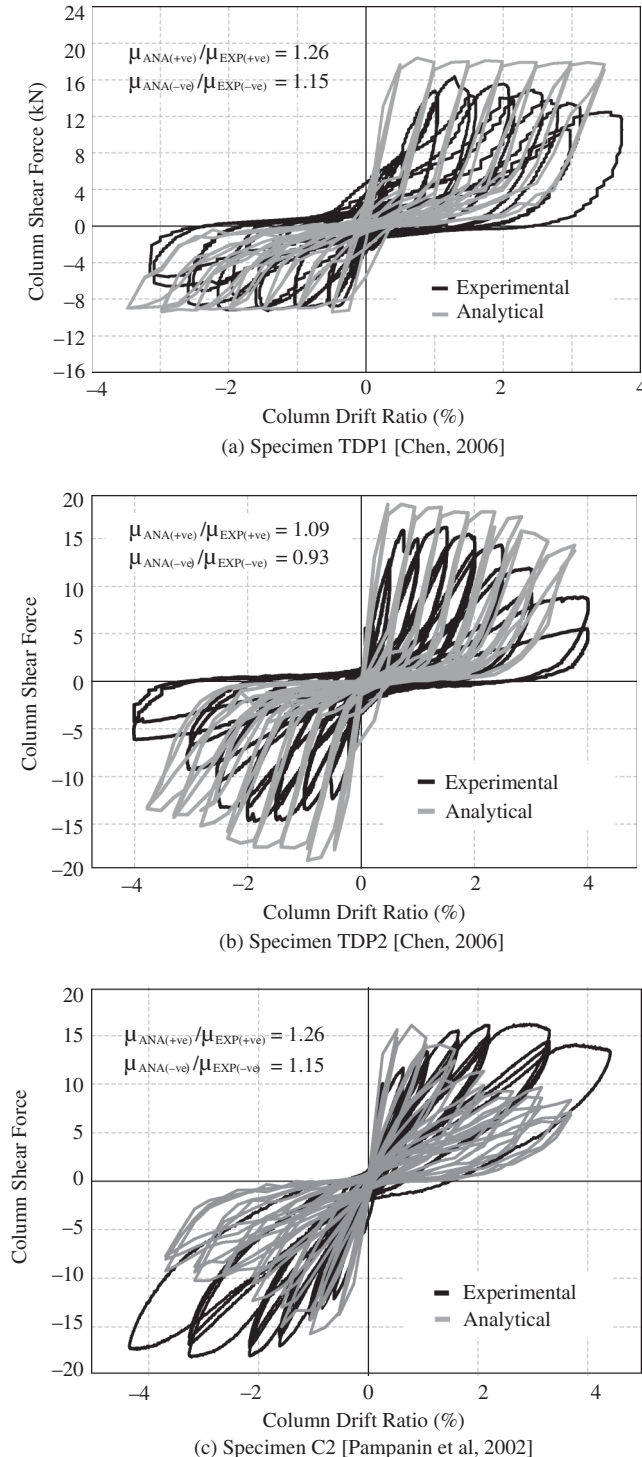


FIGURE 12 Column shear-drift response for non seismically design beam-column sub-assemblies containing smooth reinforcement.

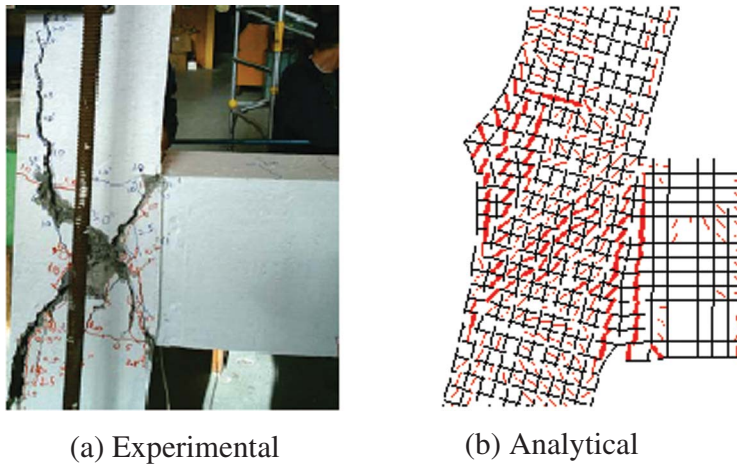
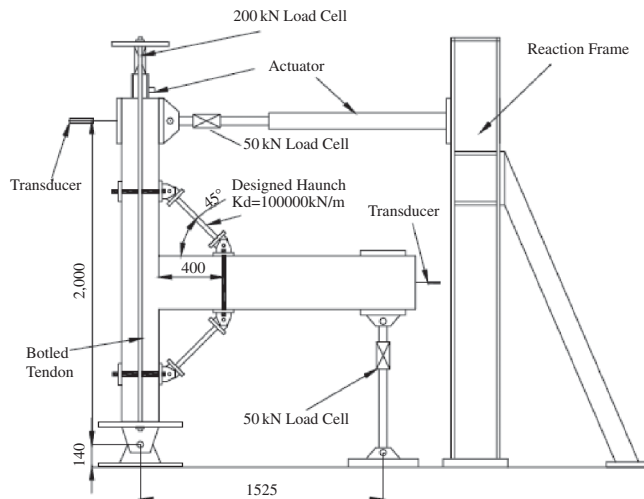


FIGURE 13 Concrete wedge failure mechanism for Specimen TDP2 [Chen, 2006] (color figure available online).

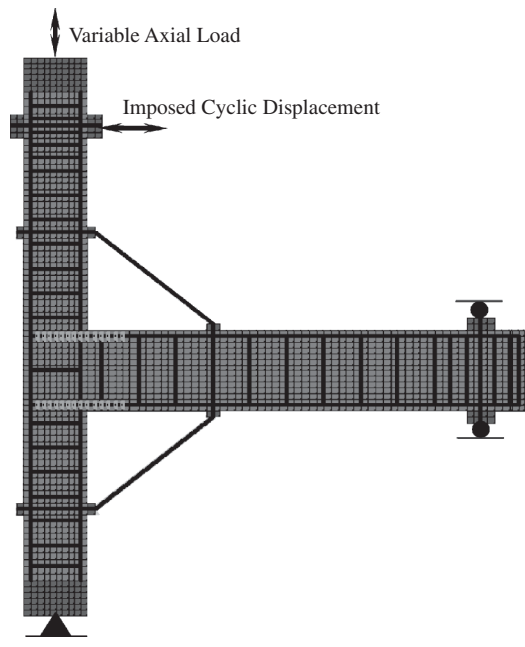
desirable ductile mechanism. In this technique, haunch bars are added to the joint panel region of the structure. The stress flow around the joint is redirected, and a designated plastic hinge region in the beam is developed [Pampanin and Christopoulos, 2003]. The brittle failure mechanisms around the joint panel regions can be prevented with the proper selection of the geometry and stiffness of the haunch elements, but capacity design considerations must be followed properly in order not to have shear failures in the structural elements. (Note: Specimen THR, prior to retrofit, was similar in design to Specimen TDP2 examined previously.) The specimen configuration and test set-up for THR is shown in Fig. 14a; the finite element model used for the analysis is illustrated in Fig. 14b.

In the experiment, plastic hinging was successfully diverted to the beam. Minor cracks were reported around the joint by Chen [2006], but the flexural crack on the beam outside the haunch area dominated the failure mechanism. (Recall that companion specimen TDP2 sustained a brittle failure mechanism with severe shear cracking in the joint panel zone.) The hysteretic response of the member was changed from a pinched behavior to a ductile and stable response; see Fig. 15a. The failure mechanism was successfully transformed from a brittle shear mechanism in the joint to a much more ductile flexural-shear mechanism in the beam.

Although this specimen contained smooth reinforcing bars for which an adequate cyclic bond-slip model does not exist, the VecTor2 analysis was able to capture the behavior of the retrofitted subassembly with a reasonably accurate load-deformation response, as seen in Fig. 15a. The progression of damage and the final failure mechanism were also accurately calculated (see Fig. 15b), as were the shear strengths and displacement ductility ratios (see Table 2). The experimental response did exhibit a more pinched response than calculated, arising from more pronounced shear damage at the location of the beam collar, and the total energy dissipation was somewhat underestimated. However, it is important to note that the finite element model used for the retrofitted THR specimen was identical to that used for the original TDP2 specimen except for the addition of the elements representing the diagonal haunch bars and collars. That the model, without modification, was able to capture a complete reversal of the beam-column joint strength hierarchy is significant.



(a) Test Set-up Showing Retrofitted Specimen [Chen, 2006].

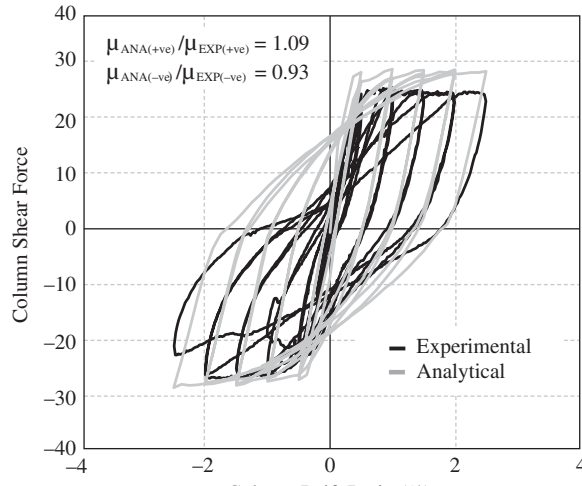


(b) Finite Element Model.

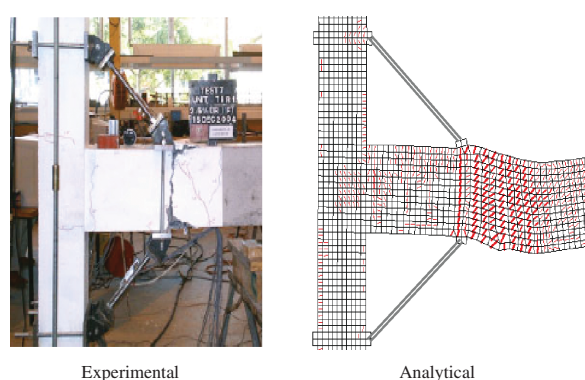
FIGURE 14 Details of retrofitted specimen THR.

10. Conclusions

An analytical investigation was carried out to investigate the effectiveness of nonlinear finite element modeling procedures in capturing the nonlinear cyclic response of beam-column subassemblies. A total of 12 experimentally tested beam-column subassemblies, spanning a range of design and loading conditions, were modeled using program VecTor2. The computed responses were examined with particular attention paid to the effects of shear deformations in the joint regions and bond-slip of the beam longitudinal reinforcement on



(a) Column Shear-Drift Responses.



(b) Failure Modes.

FIGURE 15 Behavior of retrofitted specimen THR [Chen, 2006] (color figure available online).

the hysteretic response, energy dissipation capacity, cracking and damage patterns, and failure mechanism of each specimen.

The results of the investigation suggest the following conclusions.

1. Nonlinear finite element analysis procedures can be an accurate and reliable tool in assessing the seismic performance of seismically designed and non seismically designed beam-column subassemblies. Both interior and exterior units can be modeled effectively.
2. Aspects of behavior such as hysteretic load-deformation response, strength capacity, ultimate ductility, total energy dissipation, cracking and damage progression, and failure mode can be accurately calculated. For the specimens examined, strengths and ductilities were calculated to within means of 5%, and energy dissipation to within a mean of 10%, with reasonably low scatter.
3. For accurate simulations to be achievable, the finite element package employed must contain formulations for comprehensive and realistic constitutive modeling of

various importance second-order mechanisms prevalent in the behavior of cracked reinforced concrete. Of particular importance is the rigorous modeling of concrete compression softening (for capturing joint shear damage and strength capacity), concrete tension stiffening (for energy dissipation and ductility calculations), bond slip (for anchorage loss mechanisms), confinement effects (for strength and ductility calculations), and hysteretic response of concrete and reinforcement (for energy dissipation). Most of the large multi-purpose finite element packages currently available will not have this capability, but a number of specially developed programs do.

4. The smeared rotating crack model employed in VecTor2, incorporated into a total-load secant-stiffness algorithm, represents a simple and accurate alternative procedure for the finite element modeling of cyclically loaded beam-column subassemblies. Most other programs are based on a fixed crack or microplane model for concrete, and employ an incremental-load tangent-stiffness based computation procedure.
5. An improved cyclic bond-slip model for smooth reinforcement is required in order to obtain improved simulations for non seismically designed subassemblies containing such reinforcement.
6. Finite element analysis procedures can provide accurate simulations of seismically retrofitted subassemblies, and can thus be an effective tool in investigating alternative retrofit schemes.

General guidelines for effective finite element modeling of beam-column subassemblies were established based on the outcomes of the analyses conducted. These recommendations, presented and discussed within the article, are applicable regardless of the software being used.

References

- Asatzu, N., Unjoh, S., Hoshikuma, J., and Kondoh, M. [2001] "Plastic hinge length of RC columns based on the buckling characteristics of longitudinal reinforcement," *Journal of Structure Mechanics and Earthquake Engineering, Japan Society of Civil Engineers* **682**, I-56, 177–194 (in Japanese).
- Baglin, P. S. and Scott, R. H. [2000] "Finite element modeling of reinforced concrete beam-column connections," *ACI Structural Journal* **97**(6), 886–894.
- Bertero, V. V. and Popov, E. P. [1977] "Seismic behavior of ductile moment-resisting reinforced concrete frames," *Reinforced Concrete Structures in Seismic Zones, ACI Special Publication, SP-53*, American Concrete Institute, Detroit, Michigan.
- Bond, J. [1969] "A study of reinforced concrete beam-to-column connections," M.A.Sc. Thesis, Dept. of Civil Engineering, University of Toronto, Toronto.
- Calvi, G. M., Magenes, G., and Pampanin, S. [2002] "Relevance of beam-column joint damage and collapse in RC frame assessment," *Journal of Earthquake Engineering* **6**(2), Special Issue 1, 75–100.
- Celik, O. C. and Ellingwood, B. R. [2008] "Modeling beam-column joints in fragility assessment of gravity load designed reinforced concrete frames," *Journal of Earthquake Engineering* **13**(3), 357–381.
- Chen, Te-Hsui [2006] "Retrofit strategy of non-seismically designed frame systems," Masters Thesis, Civil Engineering Dept., University of Canterbury, New Zealand.
- Dhakal, R. D., Pan, T., Irawan, P., Tsai, K., Lin, K., and Chen, C. [2005] "Experimental study on the dynamic response of gravity-load designed reinforced concrete connections," *Engineering Structures* **27**(1), 75–87.

- Elgehausen, R., Genesio, G., Ožbolt, J., and Pampanin, S. [2008] "3D analysis of seismic response of RC beam-column exterior joints before and after retrofit," *Proc. of the International Conference on Repairing, Retrofit and Rehabilitation ICRRR*, Cape Town, South Africa.
- Elgehausen, R., Ožbolt, J., Genesio, G., Hoehler, M. S., and Pampanin, S. [2006] "3D modeling of poorly detailed RC frame joints," *Proc. of the New Zealand Society for Earthquake Engineering Conference NZSEE*, March 10–12, Napier, New Zealand, Paper No. 23.
- Elgehausen, R., Popov, E. P., and Bertero, V. V. [1983] "Local bond stress-slip relationship of deformed bars under generalized excitations," *EERC Report 83-23*, Earthquake Engineering Research Center, University of California, Berkeley, California.
- Elmorsi, M., Kianoush, R. M., and Tso, W. K. [2000] "Modeling bond-slip deformations in reinforced concrete beam-column joints," *Canadian Journal of Civil Engineering* **27**(3), 490–505.
- Fabbrocino, G., Verderame, G. M., Manfredi, G., and Edoardo, C. [2004] "Structural models of critical regions in old-type RC frames with smooth rebars," *Engineering Structures* **26**(4), 2137–2148.
- Favvata, M., Izzuddin, B., and Karayannis, C. [2008] "Modeling exterior beam-column joints for seismic analysis of RC frame structures," *Earthquake Engineering and Structural Dynamics* **37**(13), 1527–1548.
- fib [2003] "Seismic assessment and retrofit of reinforced concrete buildings: state-of-the-art report," International Federation for Structural Concrete (fib), Lausanne, Switzerland.
- Filippou, F. C., Popov, E. P., and Bertero V. V. [1983] "Effect of bond deterioration on hysteretic behavior of reinforced concrete joints," *EERC Report 83-19*, Earthquake Engineering Research Center, University of California, Berkeley, California.
- Fleury, F., Reynouard, J.-M., and Merabet, O. [2000] "Multicomponent model of reinforced concrete joints for cyclic loading," *ASCE Journal of Engineering Mechanics* **126**(8), 804–811.
- Goyal, A. P. [1969] "A study of ductility of reinforced concrete beam column joints," M.A.Sc. Thesis, Dept. of Civil Engineering, University of Toronto, Toronto.
- Hegger, J., Sherif, A., and Roeser, W. [2004] "Nonlinear finite element analysis of reinforced concrete beam-column connections," *ACI Structural Journal* **101**(5), 604–614.
- Kent, D. C. and Park, R. [1971] "Flexural members with confined concrete," *ASCE Journal of Structural Division* **97**(7), 1969–1990.
- Kupfer, H., Hilsdorf, H. K., and Rusch, H. [1969] "Behavior of concrete under biaxial stress," *ACI Journal* **87**(2), 656–666.
- Limkatanyu, S. and Spacone, E. [2003] "Effect of reinforcement slippage on non-linear response under cyclic loadings of RC frame structures," *Earthquake Engineering and Structural Dynamics* **32**(15), 2407–2424.
- Lowes, N. L. and Altoontash, A. [2003] "Modeling reinforced-concrete beam-column joints subjected to cyclic loading," *ASCE Journal of Structural Engineering* **129**(12), 1686–1697.
- Mitra, N. and Lowes, L. N. [2004] "Evaluation and advancement of a reinforced concrete beam-column joint model," *Proc. of the Thirteenth World Conference on Earthquake Engineering*, August 1–6, Vancouver, B.C., Canada, Paper No. 1001.
- Mitra, N. and Lowes, L. N. [2007] "Evaluation, calibration, and verification of a reinforced concrete beam-column joint model," *ASCE Journal of Structural Engineering* **133**(1), 105–120.
- Ngo, D. and Scordelis, A. C. [1967] "Finite element analysis of reinforced concrete beams," *ACI Journal* **64**(3), 152–163.
- Palermo, D. and Vecchio, F. J. [2003] "Compression field modeling of reinforced concrete subjected to reversed loading: formulation," *ACI Structural Journal* **100**(5), 616–625.
- Pampanin, S., Calvi, G. M., and Moratti, M. [2002] "Seismic behavior of RC beam-column joints designed for gravity loads," *Proc. of the Twelfth European Conference on Earthquake Engineering*, September 9–13, London, UK, Paper No. 727.
- Pampanin, S. and Christopoulos, C. [2003] "Non-invasive retrofit of existing RC frames designed for gravity loads only," *Proc. of the fib2003 Symposium: Concrete Structures in Seismic Regions*, May 6–8, Athens, Greece, Paper No. 170.
- Pampanin, S., Christopoulos, C., and Chen, T.-H. [2006] "Development and validation of a metallic haunch seismic retrofit solution for existing under-designed RC frame buildings," *Earthquake Engineering and Structural Dynamics* **35**(14), 1739–1766.

- Pampanin, S., Magenes, G., and Carr, A., [2003] "Modeling of shear hinge mechanism in poorly detailed RC beam-column joints," *fib2003 Symposium on Concrete Structures in Seismic Regions*, Athens.
- Park, R. [2002] "A summary of results of simulated seismic load tests on reinforced concrete beam-column joints, beams and columns with substandard reinforcing details," *Journal of Earthquake Engineering* **6**(2), 147–174.
- Park, R., Priestley, M. J. N., and Gill, W. D. [1982] "Ductility of square-confined concrete columns," *ASCE Journal of Structural Division* **108**(4), 929–950.
- Richart, F. E., Brandtzaeg, A., and Brown, R. L. [1928] "A study of the failure of concrete under combined compressive stresses," *Bulletin No. 185*, University of Illinois Engineering Experimental Station, Urbana, Illinois.
- Sagbas, G. [2007] "Nonlinear finite element analysis of beam-column subassemblies," M.A.Sc. Thesis, Dept. of Civil Engineering, University of Toronto, Toronto.
- Seckin, M. [1981] "Hysteretic behavior of cast-in-place exterior beam-column-slab assemblies," Ph.D. Thesis, Department of Civil Engineering, University of Toronto, Toronto.
- Shin, M. and LaFave, J. M. [2004] "Testing and modeling for cyclic joint shear deformations in RC beam-column connections," August 1–6, Vancouver, B.C., Canada, Paper No. 0301.
- Shiohara, H. [2001] "New model for shear failure of RC interior beam-column connections," *ASCE Journal of Structural Engineering* **127**(2), 152–160.
- Shiohara, H. and Kusuhara, F. [2006] "Benchmark test for validation of mathematical models for non-linear and cyclic behavior of R/C beam-column joints," Report by Dept. of Architecture, University of Tokyo.
- Soroušian, P., Obasaki, K., and Marikunte, S. [1991] "Analytical modeling of bonded bars under cyclic loads," *ASCE Journal of Structural Engineering* **117**(1), 48–60.
- Tassios, P. T. and Vintzeleou, E. [1987] "Concrete-to-concrete friction," *ASCE Journal of Structural Division* **113**(4), 832–849.
- Vecchio, F. J. [2000] "The disturbed stress field model for reinforced concrete: formulation," *ASCE Journal of Structural Engineering* **126**(9), 1070–1077.
- Vecchio, F. J. and Collins, M. P. [1986] "The modified compression field theory for reinforced concrete elements subject to shear," *ACI Structural Journal* **83**(2), 219–231.
- Walraven, J. C. [1981] "Fundamental analysis of aggregate interlock," *ASCE Journal of Structural Division* **107**(11), 2245–2270.
- Wong, P. S. and Vecchio, F. J. [2002] "VecTor2 and FormWorks User's Manual," *Technical Report*, Dept. of Civil Engineering, University of Toronto, Toronto.